γ rays from muon capture in natural Ca, Fe, and Ni

David F. Measday* and Trevor J. Stocki†
Department of Physics and Astronomy, University of British Columbia, Vancouver, British Columbia V6T 1Z1, Canada
(Received 29 November 2005; published 24 April 2006)

A significant improvement has been made in the identification of γ rays from muon capture in natural Ca, and to a lesser extent for Fe and Ni. For calcium, capture was observed in ^{44}Ca and even ^{42}Ca, as well as the dominant ^{40}Ca. The (μ^-, ν) reaction was clearly observed in ^{40}Ca, but, as in the past, no clear identification was made in Fe and Ni. The $(\mu^-, \nu n)$ reaction was clearly observed in all nuclei, and the γ rays observed correspond better to the (γ, p) reaction than to spectroscopic factors from the $(d,^3\mathrm{He})$ or (t, α) reactions. Some $(\mu^-, \nu 2n)$ and other reactions have been observed at a lower yield.

DOI: 10.1103/PhysRevC.73.045501 PACS number(s): 23.40.−s, 36.10.Dr, 27.40.+z, 27.50.+e

I. INTRODUCTION

Muon capture in nuclei is a complex phenomenon that is far from understood. The (μ^-, ν) reaction is interesting from the point of view of obtaining transition strengths, and from studying the weak interaction itself. Most recent experiments have focused on this process. However, the $(\mu^-, \nu n)$ and $(\mu^-, \nu 2n)$ reactions are also very interesting, but from a different point of view as they indicate spectroscopic factors. It has been found, especially for the $(\mu^-, \nu n)$ reaction, that the transitions correspond quite closely to those observed in the (γ, p) reaction, but only approximately to the spectroscopic factors observed in proton knock-out reactions such as $(p,2p)$, $(e, e'p)$, as well as the $(d,^3\mathrm{He})$ or (t, α) reactions.

The present situation with regard to muon capture has recently been reviewed by Measday [1]. The experimental data are fairly sparse and in need of improvement. We shall focus on the experiments that observe the γ rays following the muon capture, which occurs via the weak interactions from the muonic 1s level. Because the mass of the muon is about 106 MeV/c^2, there is plenty of energy available when the muon is absorbed on a proton in the nucleus, and, although the neutrino takes away most of the energy, the product nucleus can be excited to 10 or 20 MeV. Thus, for medium-mass nuclides, about 20% of the time the (μ^-, ν) reaction feeds bound states in the product having the same mass as the target nucleus, but about 50% of the time a single neutron is given off, 10% of the time two neutrons are emitted, and the rest of the time more complex reactions occur, emitting protons or alphas. Each one of these reactions can produce γ rays, so quite a variety are produced. The reactions occur up to 1 μs after the muon stop, so the coincidence requirement is not very stringent in removing background from the experimental area, which is bathed in thermal neutrons, and 1-MeV neutrons are produced in the muon capture, and so add to the problems. Thus it is critical to measure the γ-ray energies with care and precision. A key advantage that we have is that the energies and branching ratios of γ rays are much better known now (and much more easily accessible from the National Nuclear Data Center). Modern γ-ray detectors are somewhat better than they used to be, but more important is that they are larger and more efficient for γ rays of a few MeV. Thus an experiment can now identify γ rays of 2 to 6 MeV, even though the yield may be fairly low. In addition, a modern accelerator like TRIUMF has a macroscopic duty cycle of 100%, so the data can be taken at a higher rate. We have thus revisited muon capture on natural Ca, Fe, and Ni. The calcium runs lasted several hours each, and the data are dependable and rare transitions were observed. The iron and nickel results were obtained as a check on backgrounds, and so were not so extensive, but turned out to be much better than existing data, so we present those results too.

There have been two experiments on calcium, both performed over 30 years ago. The first one by Pratt [2] at Carnegie Mellon was rather sketchy, and soon after there was a more detailed study at the CERN SC by Igo-Kemenes *et al.* [3]. These machines had poor duty cycles, so it is not surprising that we can improve on their results. We can compare the Ca results for the (μ^-, ν) reaction with the (p, n) reaction studied by Chittrakarn *et al.* [4]; this reaction will be very similar to the $(d,^2\mathrm{He})$ reaction, which is known to be similar to muon capture. For the $(\mu^-, \nu n)$ reaction we compare with a photonuclear experiment by Ullrich and Krauth [5], which was also available to Igo-Kemenes *et al.* [3]. More recent spectroscopic factors are available from the $(d,^3\mathrm{He})$ reaction [6–8] and have been evaluated by Singh and Cameron (see Refs. [9,10]).

For Fe and Ni, the only existing data for muon capture are those of Evans [11] at Chicago, also taken 30 years ago. His was a general survey, and few γ rays were observed, so even though our data are also limited, we extend his results, and improve on the number of γ rays observed, and thereby make more meaningful comparisons with other data, especially for the $(\mu^-, \nu n)$ reaction. In the case of natural iron, which is 91.8% ^{56}Fe, no (γ, p) data exist, and only spectroscopic factors are available from the reaction $^{56}\mathrm{Fe}(d,^3\mathrm{He})^{55}\mathrm{Mn}$ studied by Puttaswamy *et al.* [12], and the similarity is quite weak. Natural nickel is 68% ^{58}Ni and 26% ^{60}Ni, so the analysis is complex. For ^{58}Ni there are data on the (γ, p) reaction [13], and the similarity with the $(\mu^-, \nu n)$ reaction is quite marked, but not with the spectroscopic factors from the $^{58}\mathrm{Ni}(t, \alpha)^{57}\mathrm{Co}$ reaction

*Corresponding author: e-mail: measday@phas.ubc.ca
†Present address: Radiation Protection Bureau, Ottawa, Ontario, K1A 1C1, Canada.

[14], nor from the ^{58}Ni(d,^{3}He)^{57}Co reaction [15,16]. For ^{60}Ni there are no data from the (γ, p) reaction, and the similarity to the ^{60}Ni(t, α)^{59}Co reaction [14] and the ^{60}Ni(d,^{3}He)^{59}Co reaction [17,18] is again fairly poor.

II. EXPERIMENT

These data were taken at the same time as our previous data for ^{14}N [19], so we shall simply outline the technique, emphasizing only the differences. The experiment was performed on beamline M9B at TRIUMF. The beamline includes a 6-m, 1.2-T superconducting solenoid in which a 90-MeV/$c\pi^-$ beam can decay into muons. The resulting backward μ^- are then selected by a bending magnet and pass through a collimator into the experimental area. The beam rate was 2×10^5 s^{-1}, with negligible pions (<0.2%), but with about 20% electrons. Three plastic scintillation counters defined the muon beam, the counter before the target being 51 mm in diameter, and a large anticoincidence detector was placed behind the target. The counters were wrapped in aluminum foil and black electrical tape, which is made from polyvinyl chloride (PVC). (This turned out to be important.) The targets were contained in plastic containers with polyethylene walls. The Ca target was made of pure natural calcium turnings and had some oxide on the surface; it weighed 15 g. The iron target, made of iron powder with a weight of about 100 g and a surface density of about 1 g cm^{-2}, was oriented at 45° to the beam. A solid polyethylene target was also used inside a mu-metal shield. (Any muons stopping in the hydrogen are immediately transferred to carbon.) This turned out to be an embarrassingly good nickel target!

There were two HPGe γ-ray detectors at right angle to the beamline, but only the larger detector was used in this analysis; known locally as the Toronto detector, it is a p-type detector and has an efficiency of 37.5% with an active volume of 186 cm^3. It had an inbeam resolution of 3 keV at 1.2 MeV, 5 keV at 2.8 MeV, and 10 keV at 6.1 MeV, with a timing resolution of about 7 ns. The detector was surrounded by a NaI Compton suppressor, but we did not use this feature. In front of the detector was a plastic scintillator to tag charged particle events, mainly caused by electrons from the muon decay. The electronics comprised fairly standard spectroscopic amplifiers and timing filter amplifiers followed by a constant fraction discriminator. Events were defined by a pulse in the γ-ray detector above a hardware discriminator. Then the timing of the preceding muon was recorded as well as pulse heights on most scintillators. Each event was recorded by a starburst and a VAXstation 3200, and written to tape. Over 100 online histograms were kept for each target to monitor the progress of the data acquisition. The data could be reanalyzed offline, but the histograms had been well chosen. For the offline analysis we chose the total γ-ray histogram, but for the x-ray studies we can use the events in coincidence with the muon stop as well.

III. DATA ANALYSIS

The identification of a γ ray is mainly from its energy. The stability of the amplifiers was quite remarkable and the gain changed by less than 1 channel in 1000 over several days. The main effect seemed to be a slight pedestal shift. We took some care in obtaining good energy calibrations for each spectrum by using clean well-known lines to define the energy-channel relationship. A quadratic form was used, and the histograms were divided into sections. The spectra consisted of 2048 channels, and for our medium-gain spectrum at 1.3 keV per channel, the division would typically be 100–700, 700–1300, 1300–2000, and 2000–2700 keV, and for the low-gain spectrum at 5.3 keV per channel, the division would be 100–1400, 1400–2200, and 2200–10850 keV. At the lower energies the calibration was good to about 0.1 keV, but this deteriorated at the higher energies above 2 MeV, and the binning in the low-gain spectrum did not help. Typical calibration lines are given in Table I. The energies are known better than we need up to 2 MeV, but between 2.223 and 6.129 MeV there is a bit of a gap, so we had to rely on strong lines from muon capture itself, for which the energy is often not that well known. Note that we quote here the γ-ray energies, which can be slightly different from the level energies, because the recoil correction becomes significant above 2 MeV.

TABLE I. γ-ray and muonic x-ray energies taken from Measday [1], Helmer and van der Leun [20], Kessler *et al.* [21], Raman [22], Revay [23], and Fricke *et al.* [24].

Line	Energy (error) in keV	Reference
μ-mesic O($2p-1s$)	133.535(2)	[1]
μ-mesic Si($2p-1s$)	400.177(5)	[1]
Annihilation	510.9912(10)[a]	[1]
μ-mesic Ca($2p-1s$) x rays (wtd)	783.659(25)	[24]
^{56}Fe(n, n')	846.771(5)	[10]
^{60}Co	1173.228(3)	[20]
^{41}Ar	1293.586(7)	[10]
^{60}Co	1332.492(4)	[20]
$np \rightarrow \gamma d$	2223.2485(4)	[21]
^{39}K(3598–gs)	3597.3(2)	[10]
^{16}N	6129.14(3)	[1]
^{56}Fe(n, γ)	7645.55(3)	[22]
	7645.49(9)	[23]

[a]This energy is 7.7(10) eV below the mass of the electron [25].

Although the primary identification of a γ ray is via its energy, we had two subsidiary techniques. First if a level has two or more branches, we can check the existence of the others; even a limit can be helpful. If we have a marginal identification for a γ ray, we normally do not mention it here, but if we have marginal identification of two, or even better three transitions, then we consider the group as a good identification. Another check of an identification is the width of the observed line. Most background lines are narrow and have the intrinsic resolution of the detector (apart from annihilation radiation, which is always broadened). However, many muon capture lines are Doppler broadened quite noticeably because the nucleus is recoiling from the emission of the neutrino, and sometimes a neutron as well, but if the lifetime of the

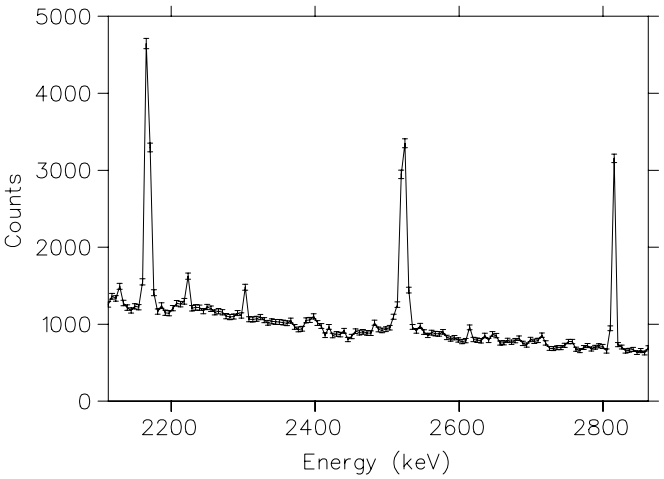

FIG. 1. A γ-ray spectrum for muon capture in natural calcium, illustrating the effects of Doppler broadening and the slowing down of the recoil ion. The peak at 2167 keV is from a level that has a lifetime of 0.47 ps, that at 2522 keV has 57 fs, and that at 2814 keV has 47 ps. The slowing down time is about a picosecond.

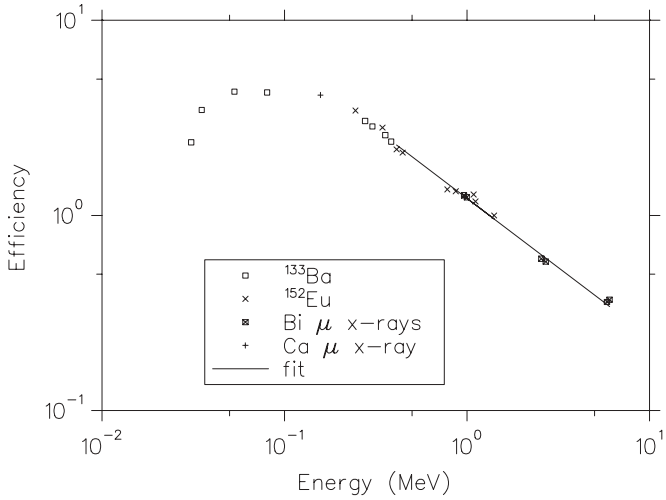

FIG. 2. The efficiency curve for our HPGe detector. We used a source of ^{133}Ba at low energy, a source of ^{152}Eu from 122 to 1408 keV, and bismuth muonic x rays at the higher energies. The Ca ($3d$-$2p$) muonic x ray is a useful point at 157 keV. Only the relative values are needed.

level is greater than about 1 ps, the recoiling ion will have stopped, producing a narrow line. This can be quite pronounced sometimes and gives us added confidence. We illustrate a typical situation in Fig. 1, which is a spectrum for calcium in the region of 2 to 3 MeV. The peak at 2167 keV is from ^{38}Ar and has a lifetime of 0.47 ps, which is an intermediate value. The peak at 2522 keV is from ^{39}K and has a short lifetime of 57 fs, whereas the peak at 2814 keV is also from ^{39}K, but the level has a long lifetime of 47 ps, and the peak is noticeably narrower.

The relative efficiency of the HPGe detector was obtained from a ^{152}Eu source for which the relative intensities are well established between 122 and 1408 keV [10,26]. The data were originally normalized to the line at 1408 keV, but in the fitting procedure, this was treated as an ordinary data point. At higher energies we used the bismuth muonic x rays and the simple relationship

$$\ln(\text{eff}) = 0.201 - 0.710 \ln E_\gamma, \qquad (1)$$

a form that has been shown to work well for most detectors. We also used a ^{133}Ba source as a check at the lower energies. Our efficiency curve is illustrated in Fig. 2. The absolute yields of the γ rays are obtained by normalizing to the muonic x rays of the target nucleus. The ($2p$–$1s$) x ray is produced for about 70 to 80% of the stops and acts as a superb normalization in the cases presented here. (For our nitrogen experiment this was a much greater problem because the x rays are at about 100 keV, which was too low.) Because the ($2p$–$1s$) x ray is produced in the same location as the γ rays, the self-absorption is taken care of to first order by the normalization procedure; it is only a few percent anyway. Furthermore, we include the intensity of the Ca($3d$–$2p$) x ray in the efficiency curve, so any energy variation is included via the efficiency correction.

We obtained our own data on the muonic cascade from the spectrum in coincidence with the stopping muon. Where comparisons can be made, our results are consistent with earlier work. In Table II we present our results for calcium, compared to those from the literature. Note that ours is a

TABLE II. The muonic Lyman series for natural calcium. The intensity of the ($2p-1s$) transition is used as an overall normalization for the muon capture data.

μ x ray	Energy[a] (keV)	Energy [24,27,28] (keV)	Intensity[a] (%)	Intensity [28,29] (%)
$2p-1s$	783.659(25)[b]	782.68(2)	83.8(10)	82.6(7)
		784.15(3)		
$3p-1s$	940.63(10)	940.70(17)	6.2(2)	6.5(3)
$4p-1s$	995.48(10)	995.40(25)	2.0(1)	2.1(2)
$5p-1s$	1020.81(10)	1020.7(3)	2.0(1)	2.1(2)
$6p-1s$	1034.62(10)	1034.4(3)	1.8(1)	1.9(2)
$7p-1s$	1042.71(20)	1043.15(30)	1.4(1)	1.2(2)
$(8-\infty)p-1s$	1046–1063[c]		2.8(4)	3.60(55)

[a]This experiment.
[b]This value is taken from Ref. [27] and used as a calibration.
[c]These energies correspond to the bump formed by the series end.

natural target, and recent experiments give x-ray energies for isotopic targets. The values of Fricke *et al*. [24] were taken from Wohlfahrt *et al*. [27], who had weighted them by the isotope abundances, then the $(2p_{3/2}–1s_{1/2})$ and $(2p_{1/2}–1s_{1/2})$ components were weighted again to give the value of 783.659(25) keV, which we used as a calibration line. It is not clear whether the Gaussian fitting program for the peaks will follow this averaging procedure in the same manner, but it is the best one can do. The energies for the Lyman series were taken from Suzuki [28], who obtained 783.85(15) keV for the (2*p*–1*s*) line. Nevertheless, our values are in excellent agreement with his and are slightly more accurate. The intensities were taken from Mausner *et al*. [29], who gave the best values for the ratio of the lines to the (2*p*–1*s*) but did not give a value for the series end (i.e., the $[(8-\infty)p-1s]$ x rays), and we had to take the value of Suzuki [28], who also gave values for the other intensities, which are reasonably compatible with those of Mausner *et al*., except for the (3*p*–1*s*) transition for which he found 5.0(3)%. Because of the adjustments we had to make to the literature values, we prefer to use our own value of 83.8(10)% for the probability of the (2*p*–1*s*) transition, though the difference is negligible in comparison to other errors.

Our values for the Lyman series in natural iron are given in Table III. We compare with the experimental values of Hartmann *et al*. [30]. We had to take their energies from their figure, so the errors are our estimate of how well we could do that, and Hartmann *et al*. bear no responsibility for that. In Table IV we present our results for the (*nd*–2*p*) series in natural calcium and compare these with the results of Suzuki [28]. The agreement is excellent. The intensity of the (3*d*–2*p*) x rays is an excellent check on the efficiency of the HPGe detector (see Fig. 2).

We present our results for the (*nd*–2*p*) series in Table V for natural iron. For the energies, Hartmann *et al*. gave no experimental values, so, for a comparison, we took the (3*d*–2*p*) observed energies and applied the same correction to the point nucleus values for the other transitions.

We obtained similar data for nickel, but because the spectra were contaminated with iron, it was difficult to separate out the various lines. However, we obtained results compatible with the iron series and used those values for normalizations.

We noticed that the chlorine (2*p*–1*s*) transition was quite prominent in several spectra, amounting to a stopping probability of about 1%. We took the opportunity to measure the energy with some care and present our results in Table VI. We believe that the best published experimental value is 578.56(30) keV and dates back to 1967 (see Backenstoss *et al*. [32] and also Acker *et al*. [33]). In their more recent compendium of muonic x rays, Fricke *et al*. [34] were forced to use the electron scattering results of Briscoe *et al*. [35], who found similar charge radii for both ^{35}Cl and ^{37}Cl. Thus our new results, even though for natural chlorine, may be more useful than at first sight.

The muonic capture constants that we used for each target are given in Table VII [36].

TABLE III. The muonic Lyman series for natural iron. The intensity of the $(2p-1s)$ transition is used as an overall normalization for the muon capture data.

μ x ray	Energy[a] (keV)	Energy [30] (keV)	Intensity[a] (%)	Intensity [30] (%)
$2p-1s$	Calib.[b]	1253.06(6)	74.5(15)	71.6(17)
	Calib.[b]	1257.19(5)		
$3p-1s$	1522.3(3)	1522(1)	7.5(4)	8.17(25)
$4p-1s$	1615.3(3)	1615.5(10)	2.7(2)	2.82(12)
$5p-1s$	1658.2(3)	1659(1)	1.6(2)	1.75(12)
$6p-1s$	1681.7(3)	1682(1)	2.2(2)	2.24(11)
$7p-1s$	1695.7(3)	1695.5(10)	2.0(2)	2.10(8)
$8p-1s$	1704.7(3)	1705.5(10)	1.2(2)	1.54(7)
$(9-\infty)p-1s$	1708–1733		8.4(10)	9.77(17)

[a]This experiment.
[b]We used these lines in the calibration, so we do not have an independent measurement.

TABLE IV. The muonic Balmer series for natural calcium. The intensity of the $(3d-2p)$ transition is used as a check on the detector efficiency.

μ x ray	Energy[a] (keV)	Energy [28] (keV)	Intensity[a] (%)	Intensity [28] (%)
$3d-2p$	157.35(13)[b]	157.45(20)	64.52(90)	66.3(15)
$4d-2p$	212.03(10)	212.05(20)	8.85(20)	8.7(3)
$5d-2p$	237.31(10)	237.10(25)	4.34(20)	3.7(2)
$6d-2p$	251.06(10)	251.05(25)	3.29(20)	2.8(3)
$7d-2p$	259.45(10)	259.35(30)	1.37(20)	1.2(3)
$(8-\infty)d-2p$	261–277		1.43(30)	1.0(4)

[a]This experiment.
[b]Calibration value averaging results taken from Engfer *et al*. [31].

TABLE V. The muonic Balmer series for natural iron.

μ x ray	Energy[a] (keV)	Energy[b] (keV)	Intensity[a] (%)	Intensity [30] (%)
$3d-2p$	265.3(3)	265.70(2)	28.8	29.4(11)
	268.9(3)	269.42(2)	16.6	15.9(6)
$4d-2p$	358.0(3)	358.0	5.4	4.8(2)
	362.0(3)	361.9	3.1	2.6(1)
$5d-2p$	400.6(3)	400.8	5.9	3.4(2)
	404.6(3)	404.8		
$6d-2p$	423.8(3)	424.0	3.4	3.0(1)
	427.8(3)	428.1		
$7d-2p$	437.8(3)	438.0	3.5	2.65(10)
	442.5(3)	442.1		
$8d-2p$	447.3(3)	447.1	1.5	1.30(5)
	451.5(3)	451.2		
$(9-\infty)d-2p$	455–475		5.9	8.55(130)

[a]Present experiment.
[b]Values from Engfer *et al*. [31], with the $(3d-2p)$ energy shift applied to the higher transitions.

TABLE VI. Values obtained for the energy of the $(2p-1s)$ muonic transition in natural chlorine. The best existing experimental value is 578.56(30) keV [32].

Run	Counts in Cl peak	Energy (keV)
Carbon-318	1000	578.81
Carbon-343	1800	578.65
Silicon	22,000	578.86
Aluminum	4000	578.83
Average		578.79(10)

IV. MUON CAPTURE RESULTS FOR ^{40}Ca

For our experiment the gate is open for 10μs after the muon stop, so there is a significant probability of including a background line in the capture spectrum. (Actually the real experiment works the other way around; after a γ ray is detected one searches for a muon stop in the delayed muon pulses.) The γ ray we detect can thus be room background from radioactive nuclei such as ^{16}N (from activated cooling water), ^{40}K, ^{41}Ar (from air activation), or ^{60}Co, or from activation by the muon beam itself (e.g., ^{56}Mn was very clear for the iron target). We also observe (n, γ) reactions from the sea of thermal neutrons at a high-energy accelerator (identifying lines from H, Na, Al, Cl, Mn, Fe, Cu, Ge, and I); $(n, n' \gamma)$ reactions from the few-MeV neutrons produced in the muon capture process hitting the target material, or material near the detector (e.g., Na, Al, Fe, and I), and especially the germanium detector itself; muonic x rays from stray muons, and finally muon capture lines from those stray muons in other elements such as Fe and Ni, which were the main problems here. Fortunately carbon and oxygen lines, though abundant, are very low in energy. Thus significant effort was expended on identifying the many background lines and estimating their contribution to a specific spectrum. Those interested in such details can study our working Excel sheets, which give our estimates for all such backgrounds [37]. A list of 300 or 400 γ rays was normal practice. As the search for rarer capture γ rays continues, this will become an even worse problem. Another difficulty is statistical fluctuations in a complex spectrum; we had two excellent spectra for ^{40}Ca of about equal quality; instead of combining them, we analyzed them independently, and we do not discuss a line unless it was clear in both spectra. This avoids fluke fluctuations, but it does not, of course, avoid real weak background lines (but we took long background runs to check those). The end result is that we believe that any identification we give here will be a genuine capture γ, but there is always the possibility of a mistake; we have found some in earlier publications and do not claim to be perfect either.

We present in Table VIII our results for muon capture in calcium, going to levels in ^{40}K. The isotope ^{40}Ca is dominant anyway (abundance of 96.94%), and the other isotopes are heavier and would produce γ rays from heavier isotopes of potassium from those we observed. We thus take our results to be those for just ^{40}Ca, and we raise the yields by 3% (a negligible correction anyway). We have used the energies of the levels and transition energies that are available at the National Nuclear Data Center at BNL [10]. The values are not always consistent, and a γ ray can sometimes have a value greater than the level energy, whereas in fact it is always smaller, though mostly very slightly. To complicate the matter further, the literature values of the branching ratios of the higher transitions changed significantly during our data analysis! Our coding for confidence of observation is that an error equal to the intensity should be interpreted as reasonable evidence, but far from certain; an error of half the observed intensity means that we are fairly confident the γ ray is present, but the statistics are poor, or there is a nearby confusing γ ray that makes it difficult to estimate the number of counts. Beyond an energy of 2808 keV we have no confident identifications for the (μ^-, ν) reaction, except for the level at 4537 keV. We have explicitly searched for 22 transitions and placed limits of about 0.3% on their intensity. We have included in the table levels near 2700 and 3900 keV because we shall need those for comparison later. We note two complications. The 1613.84-keV transition from the 1643.65-keV level is observed to be at 1612.5(2) keV (i.e., too low by over 1 keV), and this is observed independently in both spectra; we interpret this as a contribution from the 1611.27-keV transition in ^{37}Ar. We use the observed energy to allocate the yields. Similarly, we found that the 843.50-keV transition is observed to be at 843.5(1) as expected, even though it must be contaminated by the Al(n, n') line at 843.74 keV, which, from the yield of the similar line at 1014 keV, we can estimate as $\sim$60% of the observed yield. We have no explanation why the observed energy is inconsistent with this interpretation. The region is further complicated by the presence of the Fe(n, n') line at 846.75 keV.

TABLE VII. Values for the capture probabilities used for natural calcium, iron, and nickel [36].

Quantity	Calcium	Iron	Nickel
Muonic lifetime (ns)	334(2)	205.9(10)	157.0(10)
Muonic capture rate (s^{-1})	$2994(18) \times 10^3$	$4413(24) \times 10^3$	$5924(36) \times 10^3$
Decay rate (s^{-1})	448×10^3	443.8×10^3	441.1×10^3
Capture probability (%)	85.0	90.86	93.07
Target material	metal chips	metal powder	mu-metal
Number of $(2p-1s)$ x rays	1.7×10^6	16×10^3	9×10^3

TABLE VIII. γ-ray yields, per muon capture, for the reaction ^{40}Ca(μ^-, ν)^{40}K.

Level in ^{40}K (keV)	J^π	Transition branching ratio (%)	Transition energy (keV)	Observed γ-ray yield (%)
800.14	2^-	100	770.31	7.8(3)
891.40	5^-	99	891.37	0.23(10)
1643.64	0^+	81	1613.84	0.5(2)[a]
		19	843.49	0.3(2)[b]
1959.07	2^+	19	1929.34	0.31(15)
		81	1158.90	0.85(15)
2047.35	2^-	29	2047.28	0.26(10)
		31	2017.53	0.29(14)
		40	1247.17	0.35(12)
2069.81	3^-	37	2070.08	0.27(10)
		50	2039.94	0.35(17)
2103.67	1^-	71	2073.74	0.76(18)
		28	1303.53	0.30(8)
2260.40	3^+	81	2230.54	<0.2
2289.87	1^+	33	1489.77	0.11(8)
		58	646.22	0.37(15)
2290.49	3^-	83	2290.58	<0.2
		17	1399.03	<0.1
2397.17	4^-	26	2397.12	<0.4[c]
		67	2367.17	<0.2
2419.17	2^-	17	2389.18	0.1(1)
		75	1619.00	0.3(2)
2625.99	0^-	70	522.32	0.43(6)
		30	1825.77	0.16(6)
2730.37	1	82	1086.71	<0.2
2807.88	$(1, 2)^-$	95	2007.71	0.32(20)
3228.67	2^-	24	3198.6	<0.25
		40	2428.28	<0.3
		16	938.72	hidden
3868.66	2^-	44	3838.50	<0.4
		18	3068.7	<0.4
		16	1765.24	<0.25
3887.92	$(1^-, 2, 3)$	51	3857.97	<0.3
		32	3088.3(5)	<0.3
3923.90	$(1^-$ to $4^+)$	41(20)	3895.7	<0.4
4537.06	2^-	32	4506.96	<1
		47	3737.01	0.4(2)

[a]Close to the 1611.27-keV transition in ^{37}Ar; yield obtained from the observed energy.
[b]Close to the 843.74-keV transition from Al(n, n').
[c]Close to the 2398-keV transition in ^{38}Ar, which dominates.

From these observations we can deduce the direct feeding yields of specific levels, which are given in Table IX. This involves correcting for the branching ratios, and subtracting off feeding from higher levels. It is clear that there are higher level transitions that are too weak to be confidently observed, and these could contribute cascading through the lower levels. Thus the numbers listed in the column marked "known cascading" should be taken as lower limits, and thus our values for the direct yield should be used with caution, but we have to do this to compare with experiments that observe only the direct transition. The levels that are mainly affected by this uncertainty are the 800-keV level, for which at least a third of its intensity is from cascading, and the 1644-keV level, for which about half of the intensity is from cascading. We include the muon capture results of Igo-Kemenes *et al.* [3], who gave their results just in this form (not giving the actual γ-ray yields.) They also calculated the yield per muon stop, which has to be increased by a factor of 1.176 [i.e. (capture probability)$^{-1}$] to give the yield per capture (see Table VII). The comparisons in Table IX are quite satisfactory, though the measurements disagree slightly but are not wildly outside the errors. We also include the yield from the reaction ^{40}Ca(p, n)^{40}Sc observed by Chittrakarn *et al.* [4]. There are two obvious difficulties with this comparison. First, the reaction feeds the mirror nucleus, but comparisons of the (p, n) and (d,^{2}He) reactions show remarkable congruence. More seriously, the best spectrum that they present is at 4°, which is at a smaller momentum transfer than in muon capture, so we have tried to estimate the cross section at about 10°, which is at about the correct momentum transfer, but the figures are hard to decipher. Nevertheless, the comparison is helpful. The main difficulty lies in identifying the mirror levels; the resolution of the (p, n) reaction is about 220 keV, so the levels are blurred, and the levels will be at a different energy anyway. Their peak at 2700 keV in the (p, n) reaction is probably a mixture of transitions to the levels at 2626 and 2808 keV in ^{40}K, and their peak at 4300 keV in the (p, n) reaction is probably equivalent to the 4537-keV level in ^{40}K, but we could not find satisfactory matches for the peak at 3900 keV.

We present in Table X our results for the reaction ^{40}Ca(μ^-, νn)^{39}K. Again we first give the yields of the γ rays as observed. The number of lines observed is about double that of previous experiments, especially at the higher energies. The only thing to note is that the 3938.8-keV transition to the ground state is very close to a 3936.4-keV transition in ^{38}Ar, and these lines are broadened to 20 keV by the neutron emission; thus we cannot separate the γ rays, but we can use the observed energy of the combined lines to estimate the relative yields.

As before, we present in Table XI the results for direct capture to specific levels in ^{39}K with the cascading effects removed, taking into account the branching ratios. We note again that the "known cascading" should be taken as a lower limit. We include the muon capture results of Igo-Kemenes *et al.* [3], who gave their results just in this form (not giving the actual γ-ray yields). They also calculated the yield per muon stop, which has been increased by a factor of 1.176 to give the yield per capture (see Table VII).

In column 4 of Table XI, we present the results of Ullrich and Krauth, who detected γ rays from the reaction ^{40}Ca(γ, $p\gamma$)^{39}K, using 32-MeV bremsstrahlung. Their experiment produces similar yields for the reaction ^{40}Ca(γ, $n\gamma$)^{39}Ca, and the distinction between theses reactions is based on energy alone; however, as the resolution of the γ rays is 50 keV or more because of the Doppler broadening as well as the small Ge(Li) detector, the identification of a γ ray is not always unique. Nonetheless, as noted by Igo-Kemenes *et al.*, the comparison between muon capture and the ^{40}Ca(γ, $p\gamma$)^{39}K reaction [5] shows great similarity, whereas the spectroscopic factors [8,10] are not a good predictor of what we observe

TABLE IX. Yields for muon capture to specific levels in ^{40}K with the cascading effects removed, compared to the earlier results of Igo-Kemenes *et al*. [3], all given as yield per capture. Also a comparison is made to the reaction ^{40}Ca$(p, n)^{40}$Sc from Chittrakarn *et al*. [4] at about 10° in the lab.

Level in ^{40}K (keV)	Known cascading (%)	Direct yield per capture[a] (%)	Direct yield per capture [3] (%)	Yield in the reaction ^{40}Ca$(p, n)^{40}$Sc [4]	Level in ^{40}Sc (keV)
0				∼0	0
29.83				∼0	34
800.14	2.8(5)	5.0(5)	4.2(1.2)	1.3	772
891.40	0.03(2)	0.2(1)			
1643.64	0.37(15)	0.5(4)			
1959.07	0.04(2)	1.2(2)	0.5(2)	0.25	1799
2047.35		0.9(3)	0.53(18)		
2069.81		0.7(3)			
2103.67	0.43(6)	0.7(2)			
2260.40		<0.25			
2289.87		0.5(2)			
2290.49		<0.24			
2397.17		<0.3			
2419.17		0.4(3)	1.53(24)		
2625.99		0.60(8)			
2730.37		<0.24		0.35	∼2700
2807.88		0.34(21)			
3228.67		<0.8			
3868.66		<0.9		0.15	∼3900
3887.92		<0.6			
3923.90		<1.0			
4537.06		0.85(42)		0.4	∼4300

[a]This experiment.

in muon capture. This conclusion is even stronger now that we have significantly extended the number of γ rays observed in muon capture, although the contamination by ^{39}Ca γ rays in the study by Ullrich and Krauth [5] weakens the comparison. There are many other reactions in which a proton is knocked out of ^{40}Ca, such as $(p,2p)$, $(e, e'p)$, or high-energy (γ, p); these all give better agreement with the spectroscopic factors, though the energy resolution is not sufficient to be useful to us. An example of this frustrating situation is the (γ, p) experiment of van den Abeele *et al*. [38], who used tagged photons of 60 MeV, but their energy resolution of 300 keV means that only a general comparison can be made, even though this is an excellent resolution for this type of experiment. Similarly, the experiment of Kramer *et al*. [39] on ^{40}Ca$(e, e'p)$ yielded a resolution of 130 keV, and the observed energy levels agree better with the spectroscopic factors.

More than one neutron can be emitted at muon capture. For heavy elements as many as four, five, or even six neutrons are observed. For lighter elements multiple neutron emission is not so common. We present our results for ^{40}Ca$(\mu^-, \nu 2n)^{38}$K and ^{40}Ca$(\mu^-, \nu 3n)^{37}$K in Table XII, and we compare these to the strength of the reaction ^{40}Ca$(d, \alpha)^{38}$K [40], taking the values from a single spectrum at 120°, and normalizing to the strongest line feeding the 459-keV level.

We see that apart from the 328-keV transition in ^{38}K, the observations are quite marginal. We also note a slight disagreement with the result of Igo-Kemenes *et al*. concerning the transition at 1567.9 keV. The situation is illustrated in Fig. 3. We observe that there is a peak at 1562.69 keV from

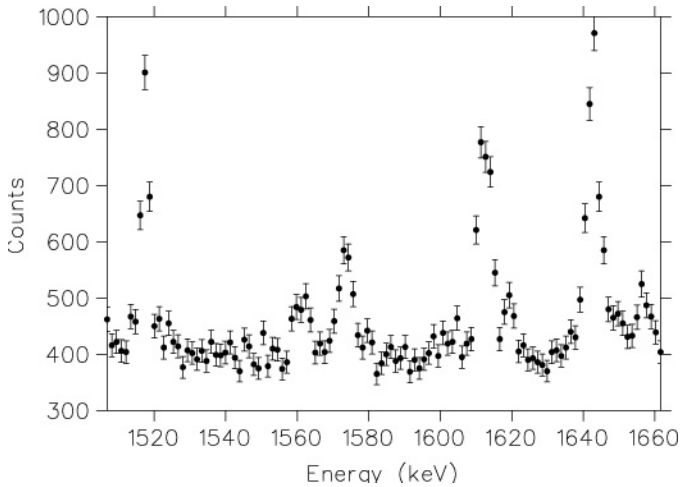

FIG. 3. A γ-ray spectrum from muon capture in natural calcium, illustrating a new identification for the peak around 1570 keV. Igo-Kemenes *et al*. [3] interpreted the yield as coming from a 1567.9-keV line in ^{38}K. We believe that a better attribution is a combination of a transition in ^{39}Ar at 1562.69 keV, and another in ^{39}K at 1572.8 keV. [Note that the peak at 1517.51 keV is from a level in ^{39}Ar, which (unusually at this energy) has a very long lifetime of 0.95 ns, so the peak exhibits no Doppler broadening.]

TABLE X. γ-ray yields, per muon capture, for the reaction ^{40}Ca(μ^-, νn)^{39}K.

Level in ^{39}K (keV)	J^π	Transition branching ratio (%)	Transition energy (keV)	Observed γ-ray yield (%)
2522.5	$1/2^+$	100	2522.4	6.7(5)
2814.3	$7/2^-$	100	2814.2	4.0(2)
3019.2	$3/2^-$	100	3019.1	2.8(3)
3597.5	$9/2^-$	54	3597.3	0.35(11)
		46	783.2	hidden
3883.1	$5/2^-$	100	3882.9	0.7(3)
3938.8	$3/2^+$	92	3938.6	1.0(3)[a]
		8	1416.3	<0.1
3944.3	$11/2^-$	63	1130.0	0.12(6)
		37	346.8	hidden
4082.3	$3/2^-$	67	4082.1	0.80(25)
		21	1559.8	0.16(8)
		12	1063.1	<0.1
4095.3	$1/2^+$	85	1572.8	0.76(20)
4126.0	$7/2^-$	100	1311.7	0.3(2)
4475.1	$(1/2, 3/2)^-$	37	4474.8	<0.5
		47	1952.5	0.2(1)
		16	1455.9	0.07(4)
4930.1	$3/2^+$	76	4929.8	<0.6
		24	2407.5	<0.3
5163.9	$9/2^-$	55	1219.6	<0.35
5165.5	$(5/2,7/2,9/2)^-$	100	2351.1	<0.3
5173.4	n.a.[b]	100	5173.0	<0.4
5262.7	$5/2^+$	100	5262.3	1.0(2)
5318.2	$3/2^+$	100	5317.8	0.55(20)
5597.9	$5/2^+$	100	5597.5	0.4(2)
5826.3	$1/2^-, 3/2^-$	100	5825.8	hidden
5891	$7/2^-$	71	3077	<0.4
5937.9	$5/2^+$	100	5937.4	<0.5
6331.0	$3/2^+$	100	6330.4	1.1(3)
6356	$5/2^+$	?	6355	<0.5
		?	2473	<0.2
>6381			proton unbound	
>13077			neutron unbound	

[a]Close to the 3936-keV transition in ^{38}Ar; yield obtained from the observed energy.
[b]n.a.: not available.

^{39}Ar [yield of 0.28(15)%] and another peak at 1572.8 keV from ^{39}K (see Table X), which is quite strong with a yield of 0.76(20)%.

We believe that these are much better identifications than a line in ^{38}K at 1567.9 keV, and we observe no convincing evidence for it. Note that, in Fig. 3, the peak at 1517.51 keV is from a level in ^{39}Ar, which has a long lifetime of 0.95 ns and the peak is narrow, whereas the peak 1642.71 keV is a transition from the 3810.1-keV level in ^{38}Ar, which has a short lifetime of 55 fs and is noticeably broadened. (The peak at 1612 keV is a mix of several γ rays.) Note also that the peaks at 1563 and 1573 keV are somewhat broadened. The 1573-keV peak is from ^{39}K with a lifetime of 63 fs, so should be broadened, but the peak at 1563 keV is a transition from the 2830-keV level in ^{39}Ar, which has a lifetime of >0.7 ps; it seems that the apparent broadening is a statistical fluctuation.

The comparison to the reaction ^{40}Ca(d, α)^{38}K is of uncertain value. The numbers are just the strength at one angle and energy, so they are probably a poor predictor for the yield in muon capture but may give a general indication. A more useful comparison would be to the reaction ^{40}Ca(π^-,$2n$)^{38}K for stopping π^-, but unfortunately the experiment of Engelhardt *et al.* [41] identified only one γ ray from ^{38}K, the one at 2646 keV, which we do not observe. In other targets they detected two or three lines for this reaction, which shows that it would be interesting to pursue this comparison. The trouble is that a π^- induces many complex reactions and produces a multitude of γ rays.

In muon capture there can be more complex reactions involving emission of protons, α, and deuterons. We cannot distinguish the ^{40}Ca(μ^-, νpn)^{38}Ar reaction from the ^{40}Ca(μ^-, νd)^{38}Ar reaction, but charged particle detection has indicated that the ratio is about 2:1 [1]. Now the nucleus ^{40}K is rather unusual in that the particle emission thresholds are inverted from the normal pattern, thus it emits alphas at an excitation of 6.44 MeV, protons at 7.58 MeV, and neutrons at

TABLE XI. Yields for muon capture to specific levels in ^{39}K with the cascading effects removed, compared to the earlier results of Igo-Kemenes *et al*. [3], all given per muon capture. We also compare to the reaction ^{40}Ca(γ, $p\gamma$)^{39}K [5] and to the spectroscopic factors from the ^{40}Ca(d,^{3}He)^{39}K reaction [10,38].

Level in ^{39}K (keV)	Known cascading (%)	Direct yield per capture[a] (%)	Direct yield per capture [3] (%)	Yield in the reaction ^{40}Ca(γ, $p\gamma$)^{39}K [5] (MeV mb)	Spectroscopic factors from ^{40}Ca(d,^{3}He)^{39}K
0					2.20
2522.5	1.21(24)	5.5(5)	7.8(5)	57	1.66
2814.3	0.72(23)	3.3(3)	3.9(4)	15[b]	0.32
3019.2	0.20(5)	2.6(3)	1.9(4)	7[b]	0.05
3597.5	0.07(3)	0.6(2)			
3883.1		0.7(3)	0.9(2)	1.5[b]	0.02
3938.8		1.1(3)	<11?	2.5[b]	
3944.3		0.2(1)	<11?		
4082.3		1.1(3)			
4095.3		0.89(24)			0.2
4126.0		0.3(2)			
4475.1		0.43(22)			
4930.1		<0.8	<2.4	2.0	
5163.9, 5165.5, 5173.4		<1.3		3.0[b]	
5262.7		1.0(2)	0.47(24)	3.8	1.38
5318.2		0.55(20)		visible	
5597.9		0.4(2)	0.47(24)	1.6[c]	0.98
5826.3		hidden			0.05
5891		<0.6			
5937.9		<0.5		1.0[c]	0.30
6331.0		1.1(3)		2.0[c]	1.57
6356		<1			
>6381		proton unbound	proton unbound	proton unbound	
>13077		neutron unbound	neutron unbound	neutron unbound	

[a]This experiment.
[b]These yields contain significant contributions of γ rays from ^{39}Ca.
[c]There is some uncertainty of the identification of these yields. We present the most likely attribution.

TABLE XII. Muon capture γ rays from the reactions ^{40}Ca(μ^-, $\nu 2n$)^{38}K and ^{40}Ca(μ^-, $\nu 3n$)^{37}K, presented as yield per muon capture, with a comparison to the reaction ^{40}Ca(d, α)^{38}K [40].

Level (keV)	J^π	Transition branching ratio (%)	Transition energy (keV)	Observed γ-ray yield (%)	Previous results [3] (%)	(d, α) strength [39]
^{38}K						
0	3^+					55
130.4	0^+					3
458.7	1^+	100	328.3	0.5(1)	0.59(24)	100
1698.3	1^+	100	1567.9	<0.2	1.06(24)	45
2402.4	2^+	94	1943.6	0.15(10)		7
2612.9	3^-	100	2612.8	<0.3		34
2646.1	4^- (2^-)	98	2646.0	<0.25		62
^{37}K						
1370.85	$1/2^+$	100	1370.82	<0.2		
1380.25	$7/2^-$	100	1380.22	<0.3		
2170.18	$3/2^-$	87	2170.11	<0.7		
2285.24	$7/2^+$ ($5/2^+$)	100	2285.16	<0.2		
2750.27	$5/2^+$	98	2750.16	<0.2		

TABLE XIII. γ-ray yields for the reaction ^{40}Ca(μ^-, νp)^{39}Ar, given as yield per muon capture.

Level in ^{39}Ar (keV)	J^π	Transition branching ratio (%)	Transition energy (keV)	Observed γ-ray yield (%)
1267.21	$3/2^-$	100	1267.19	3.6(3)
1517.54	$3/2^+$	46	1517.51	1.05(20)
		54	250.33	hidden
2092.75	$5/2^-$	96	2092.69	0.8(2)
2342.2	$(5/2 \text{ to } 9/2)^-$	100	2342.1	<0.3
2358.28	$1/2^+$	95	1091.06	0.4(1)
2433.48	$3/2^-$	71	1166.25	0.22(17)
2481.49	$7/2^-$	83	2481.40	<0.3
2503.42	$(3/2, 5/2)^+$	93	985.86	0.57(15)
2523.74	$(5/2 \text{ to } 9/2)^-$	100	2523.65	hidden
2631.56		81	538.81	0.2(1)
2775.5	$5/2^-$	56	2755.4	<0.3
		44	1488.3	<0.2
2829.94	$1/2^+$	49	1562.69	0.28(15)
		43	1312.37	0.28(20)
2949.95	$(3/2^+, 5/2)$	49	1432.38	0.28(7)
		51	446.53	0.26(7)
3265.6	$(3/2^-)$	98	1998.3	<0.3
3287.0	$1/2^+$	100	2019.7	0.4(2)

TABLE XIV. γ-ray yields for the reactions ^{40}Ca(μ^-, νpn)^{38}Ar and ^{40}Ca(μ^-, $\nu p2n$)^{37}Ar, given as yield per muon capture.

Level (keV)	J^π	Transition branching ratio (%)	Transition energy (keV)	Observed γ-ray yield (%)
^{38}Ar				
2167.47	2^+	100	2167.41	6.6(5)
3377.45	0^+	93	1209.96	0.54(20)
3810.22	3^-	100	1642.71	2.0(2)
3936.65	2^+	93	3936.43	0.1(1)[a]
		7	1769.13	<0.16
4479.96	4^-	100	669.73	0.96(9)
4565.4	2^+	96	2397.8	0.26(13)[b]
4585.86	5^-	90	105.9	below threshold
4710.3	0^+	100	773.6	<1
5157.3	2^+	53	2989.7	<0.4
		22	1220.6	<0.2
5349.5	4^+	61	3181.9	<0.2
		31	1412.8	<0.1
5552.21	$(1,2)^+$	27	3384.58	<0.2
		40	1615.52	<0.2
		21	986.80	<0.2
^{37}Ar				
1409.82	$1/2^+$	100	1409.79	0.25(12)
1611.27	$7/2^-$	100	1611.23	0.64(20)[c]
2217.1	$7/2^+$	100	2217.0	0.12(12)
2490.6	$3/2^-$	93	2490.5	0.14(7)
2796.1	$5/2^+$	98	2796.0	0.1(1)

[a]Close to the 3939-keV transition in ^{39}K; yield obtained from observed energy.

[b]Close to the 2397-keV transition in ^{40}K, but another transition indicates that the yield of the 2397-keV transition is <0.15%.

[c]Close to the 1614-keV transition in ^{40}K; yield obtained from observed energy.

7.80 MeV; thus certain levels excited in muon capture decay mainly by α or proton emission and thus enhance the yield of such reactions. We present in Table XIII the γ-ray yields for the reaction ^{40}Ca(μ^-, νp)^{39}Ar and in Table XIV the γ-ray yields for the reactions ^{40}Ca(μ^-, νpn)^{38}Ar and ^{40}Ca(μ^-, $\nu p2n$)^{37}Ar.

From these yields we can deduce the direct feeding of the various levels and we compare our results with those of Igo-Kemenes *et al*. in a simplified manner in Table XV. For ^{37}Ar all the transitions are to the ground state, and Igo-Kemenes *et al*. had no information for this isotope.

We observe a few minor differences from the results of Igo-Kemenes *et al*. For ^{39}Ar, our direct yield for the 1517.54 keV level is somewhat lower, but this is caused by our new observation of transitions from the 2503-, 2829-, and 2949-keV levels to the 1517.54-keV level, so we have to subtract off these contributions to obtain the direct feeding. For the 2433.48-keV level, we obtain a lower yield; the observed transition is at 1166.25 keV, which is very close to a transition in ^{36}Cl at 1164.87 keV. We estimate that the ^{36}Cl transition is much stronger; the source of this transition is not clear and we estimate that most is from the reaction ^{35}Cl(n, γ), not from muon capture. For ^{38}Ar, we have no explanation for the discrepancy concerning the 3377.45-keV level; for the 3810.22-keV level, we have observed a strong cascade from the 4479.96-keV level, so our γ yields are probably compatible. For the 3936.65-keV level, the ground-state transition is very close to the 3938.8-keV level in ^{39}K, which also has a direct transition to the ground state; remember that these γ rays are broadened to 20 keV by the emission of neutrons, so the overlap is almost complete, and therefore we use the observed energy to allocate the yield to each transition. It looks as though Igo-Kemenes *et al*. had similar concerns, but they did not discuss the problem explicitly.

The isotopes of chlorine are an interesting sideline—and probably not of major interest. However, we need to give some conclusions. Our yields are presented in Table XVI.

One would not expect significant yields from the reactions ^{40}Ca(μ^-, $\nu 2p$)^{38}Cl and ^{40}Ca(μ^-, $\nu 2pn$)^{37}Cl. However, Igo-Kemenes *et al*. gave a yield of 1.24(20)% for the 1309-keV level in ^{38}Cl. We have therefore presented our results for these isotopes to show that our reduced observation is reasonable. Our result from the 638-keV transition from this 1309-keV level is <0.25%, which gives <0.33% for the excitation of the level, and the other transitions are consistent with that. (Note that the 553.6-keV transition, for which we observed a limit of <0.3%, goes to the 755.4-keV level, for which we observe a limit of <0.1% in a clean region; thus around 554 keV there is probably a background contribution, but this also confirms our nonobservation of the 638-keV transition.) All our other observations in ^{37}Cl and ^{38}Cl are marginal and as limits would be around 0.2%. We therefore believe that Igo-Kemenes *et al*. were detecting a background line [and we do not fully understand their footnote (c), which states "assuming a 100%

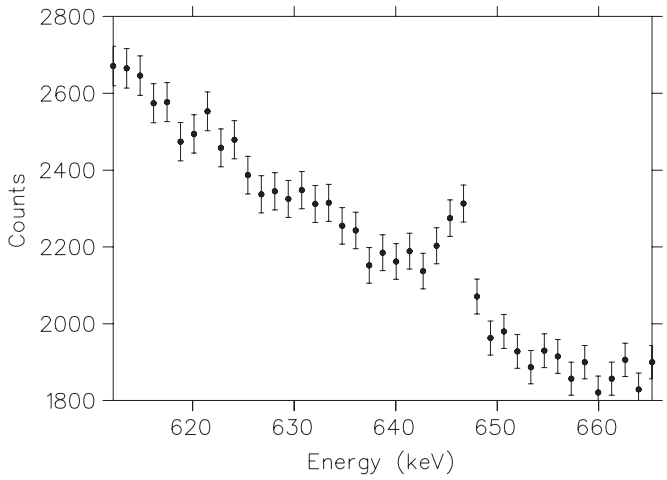

FIG. 4. A γ-ray spectrum from muon capture in natural calcium, indicating that we do not observe the 638-keV transition in ^{38}Cl. For orientation, the peak at 646 keV is from a transition in ^{40}K, which has a yield of about 0.4%.

cross-over decay", which presumably means that, at that time, the 1309-keV transition was considered to be the only decay of this level]. Our spectrum around 640 keV is illustrated in Fig. 4. The ^{38}Cl transition at 637.68 keV is not observed; for orientation the peak at 646 keV is a transition in ^{40}K, which has a yield of 0.37(15)% (i.e., a factor of 3 smaller than would be needed to equal the claimed observation by Igo-Kemenes *et al.*).

TABLE XV. Yields for muon capture to specific levels in the Ar isotopes from the reactions ^{40}Ca(μ^-, νpn)^{38}Ar and ^{40}Ca(μ^-, $\nu p2n$)^{37}Ar, with the cascading and branching ratio effects removed, compared to the earlier results of Igo-Kemenes *et al.* [3], all given as yield per muon capture.

Product nucleus	Level (keV)	Known cascading (%)	Direct yield per capture[a] (%)	Direct yield per capture [3] (%)
^{39}Ar	1267.21	2.54(40)	1.1(5)	1.2(3)
	1517.54	1.16(26)	1.1(5)	3.1(7)
	2092.75	0.2(1)	0.6(3)	0.8(2)
	2342.2		<0.3	
	2358.28		0.4(1)	0.6(2)
	2433.48		0.3(2)	0.90(15)
	2503.42	0.26(7)	0.35(17)	
	2613.56		0.25(12)	
	2829.94		0.61(26)	
	2949.95		0.54(10)	
	3265.6		<0.3	0.38(22)
	3287.0		0.4(2)	
^{38}Ar	2167.47	2.8(3)	3.8(6)	3.6(5)
	3377.45		0.58(22)	1.11(19)
	3810.22	0.96(9)	1.04(22)	1.79(18)
	3936.65		0.11(11)	1.42(+20, −80)
	4479.96		0.96(9)	
	4565.4		0.27(13)	
	5157.3		<0.8	
	5349.5		<0.3	
	5552.21		<0.5	

[a]Present experiment.

TABLE XVI. Observed yields for the reactions ^{40}Ca(μ^-, $\nu 2p$)^{38}Cl, ^{40}Ca(μ^-, $\nu 2pn$)^{37}Cl, ^{40}Ca(μ^-, $\nu\alpha$)^{36}Cl, ^{40}Ca(μ^-, $\nu\alpha n$)^{35}Cl, and ^{40}Ca(μ^-, $\nu\alpha 2n$)^{34}Cl, all given as yield per muon capture.

Nuclide	Level (keV)	J^π	Transition branching ratio (%)	Transition energy (keV)	Observed γ-ray yield (%)
^{38}Cl	755.42	3^-	100	755.42	<0.1
	1309.05	4^-	7	1309.02	<0.17
			76	637.68	<0.25
			17	553.62	<0.3
	1617.41	3^-	28	861.98	<0.2
			50	308.36	hidden
^{37}Cl	1726.58	$1/2^+$	100	1726.54	<0.15
	3086.14	$5/2^+$	100	3086.00	<0.3
	3103.50	$7/2^-$	100	3103.36	0.2(2)
	3626.82	$3/2^+$	57	3626.63	<0.2
			43	1900.19	<0.2
^{36}Cl[a]	788.44	3^+	100	788.43	<2
	1164.89	1^+	100	1164.87	0.4(4)
	1601.12	1^+	21	436.22	0.1(1)
			78	1601.08	0.1(2)
	1951.20	2^-	60	1951.15	−0.1(2)
			33	786.30	<2
	1959.41	2^+	95	1959.35	0.1(2)
	2863.96	3^+	91	2863.84	<0.3
^{35}Cl	1219.44	$1/2^+$	100	1219.42	<0.3
	1763.15	$5/2^+$	100	1763.10	0.5(3)
	2645.6	$7/2^+$	91	2645.5	<0.2
	2693.6	$3/2^+$	79	2693.5	<0.2
^{34}Cl	461.00	1^+	100	461.00	0.10(5)
	665.55	1^+	100	665.54	<0.1
	1230.28	2^+	29	1083.90	<0.15
			35	769.27	hidden
			36	564.72	0.08(8)

[a]This nucleus can be reached via the background reaction ^{35}Cl(n, γ) on the PVC tape on the counters. We have subtracted off the estimated contribution of this reaction.

For ^{36}Cl, one would expect some observable yield, but unfortunately the γ rays can also be produced by the reaction ^{35}Cl(n, γ)^{36}Cl, which we observe clearly in our background run, coming probably from the PVC electrical tape used in the construction of the plastic scintillators. In principle it is easy to separate the two sources as the thermal neutron capture produces γ rays at 3061.85, 5715.24, 6110.92, and 7414.07 keV, which are from the capturing state, and so would not be expected in our muon capture reaction. The trouble is that the statistical accuracy on those high-energy lines is quite marginal, so we have to take a 100% error on the estimated contribution from thermal capture. This we have already subtracted from the yields in Table XVI. We are left with a marginal observation of the 1165-keV level but no others. (The capture γ-ray energies that we quote are the average of those of Krusche *et al.* [42] and Kennett

et al. [43]. Note that Table II of Krusche *et al*. incorrectly states that the γ-ray energies are recoil corrected to give the level energy differences; in fact they are the observed energies.) We should note that there is no such background problem for ^{38}Cl because ^{37}Cl is only 24% natural chlorine, and the thermal neutron cross section is only 0.43 b, whereas ^{35}Cl is 76% natural chlorine, and it has an enormous thermal neutron cross section of 43 b. Returning to muon capture, we note that the (αn) production is often comparable to α production, but we observe a total yield of only $\sim$0.5% in ^{35}Cl and only marginal observations in ^{34}Cl. Remember that we cannot observe muon capture to the ground state of any of these nuclei, and it would probably be the largest contribution.

Let us now summarize the results for ^{40}Ca. For the (μ^-, ν) reaction, we observe a yield of about 12%, and we know that the ground and first excited state will not contribute substantially. For the $(\mu^-, \nu n)$ reaction, we observe a yield of 20% and estimate 8% for the ground state transition, totaling 28%. For the $(\mu^-, \nu 2n)$ reaction, we observe a yield of only 0.65% and estimate about 0.35% for the ground-state transition, totaling $\sim$1%. For the reactions producing protons or deuterons [e.g., the $(\mu^-, \nu p)$, $(\mu^-, \nu pn)$, and $(\mu^-, \nu p2n)$ reactions], we observe yields of 5.7%, 6.8%, and 1.3%, and estimating ground-state contributions to be about 10%, we reach 24%. Estimating $(\mu^-, \nu\alpha)$-type reactions to be about 3%, we obtain a sum of 68% (i.e., we are missing 32%, which is actually quite an achievement). Using the known neutron multiplicities in muon capture as a guide (Table 4.7 of Ref. [1]), we can estimate that the missing yield is probably about 15% for the (μ^-, ν) reaction, 15% for the $(\mu^-, \nu n)$ reaction, and 2% for the $(\mu^-, \nu 2n)$ reaction mainly coming from transitions that produce high-energy γ rays.

V. RESULTS FOR ^{40}Ca AND ^{42}Ca

The calcium target was of natural isotopic composition (96.94% ^{40}Ca, 0.647% ^{42}Ca, and 2.09% ^{44}Ca, with smaller contributions from even less abundant isotopes). As surprising as it may seem, we saw clear evidence for the $(\mu^-, \nu n)$ reaction from muon capture on ^{42}Ca and ^{44}Ca. We present the results in Table XVII, giving the yield for natural calcium, and then the calculated yield if the target were purely of the appropriate isotope. The yields are quite large, but even larger values have been found in other elements. The spectroscopic factors for ^{41}K and ^{43}K are also presented in Table XVII, taken from the $(d, ^3\mathrm{He})$ reaction [7,10], but the values from the (t, α) reaction are quite consistent [10,44,45]. The comparison is satisfying. Notice the large values for the ground-state transitions.

VI. RESULTS FOR ^{nat}Fe AND ^{nat}Ni

As we have already indicated, we have some results for natural iron and nickel. For iron, a short run was taken intentionally, and the results are quite clear because the isotope ^{56}Fe has an abundance of 91.8% and dominates the spectrum. The other isotopes would be below our threshold for detection. We observe transitions in ^{55}Mn from the reaction $^{56}\mathrm{Fe}(\mu^-, \nu n)^{55}\mathrm{Mn}$, which is the dominant reaction, with a few observations of ^{53}Mn, ^{54}Mn, and ^{56}Mn; we shall discuss these in detail. For nickel, we took a carbon run (using the polyethylene target), which was dominated by capture in the mu-metal shield, yet the x rays and γ rays from muon capture in nickel are so clear that we can present our observations without any problem. Nickel has two major isotopes: ^{58}Ni with an abundance of 68.3% and ^{60}Ni with an abundance of 26.1%. The other isotopes have too small an abundance to affect our results. We observe transitions in the dominant reactions of $^{58}\mathrm{Ni}(\mu^-, \nu n)^{57}\mathrm{Co}$ and $^{56}\mathrm{Ni}(\mu^-, \nu n)^{55}\mathrm{Co}$.

We present our results for iron in Table XVIII and compare these with the earlier results of Evans [11]. Our results confirm the observations of Evans, but we detect many more transitions. We do not include the 846.771-keV level in ^{56}Fe, as it is clearly a background line. (We observe it in the calcium spectrum and most others too.) The observation of lines in ^{56}Mn is questionable, so we are back to the difficulty facing early

TABLE XVII. Observed yields for the reactions $^{42}\mathrm{Ca}(\mu^-, \nu n)^{41}\mathrm{K}$ and $^{44}\mathrm{Ca}(\mu^-, \nu n)^{43}\mathrm{K}$ for the natural target, and the calculated yield for a pure isotopic target, all given as yield per muon capture. Also included are the spectroscopic factors obtained from the $^{42}\mathrm{Ca}(d, ^3\mathrm{He})^{41}\mathrm{K}$ and $^{44}\mathrm{Ca}(d, ^3\mathrm{He})^{43}\mathrm{K}$ reactions [7].

Level (keV)	Transition branching ratio (%)	Transition energy (keV)	γ-ray yield in natural calcium (%)	γ-ray yield in isotopic target (%)	C^2S for ^{41}K or ^{43}K [7]
^{41}K					
0					3.43
980.48	100	980.46	0.14(7)	22(11)	0.77
1293.61	100	1293.59	hidden		0.93
^{43}K					
0					3.15
561.2	100	561.4	0.3(1)	14(5)	1.15
738.1	100	738.1	0.45(12)	22(6)	0.85
975.0	96	974.9	0.2(1)	10(5)	0.16
1110.3	70	1110.1	<0.2	<10	0.36
	30	548.5	<0.1	<5	

TABLE XVIII. Observed γ-ray yields per muon capture in ^{nat}Fe, which is 91.8% ^{56}Fe, so the dominant reactions are ^{56}Fe(μ^-, νn)^{55}Mn, ^{56}Fe(μ^-, $\nu 2n$)^{54}Mn, and ^{56}Fe(μ^-, $\nu 3n$)^{53}Mn, and these yields should be raised by 1.089 (= 1/0.918) to obtain the yields for a pure isotopic target of ^{56}Fe. (We use level and transition energies as given by the National Nuclear Data Center [10], even if they are illogical, i.e., the transition energy is greater than the level energy). We compare to the earlier results of Evans [11].

Nuclide	Level (keV)	J^π	Transition branching ratio (%)	Transition energy (keV)	Observed γ-ray yield[a] (%)	Observed γ-ray yield [11] (%)
^{53}Mn	377.86	$5/2^-$	100	377.88	2.2(3)	1.6(5)
	2706.76	$1/2^-$	100	1416.8	0.2(2)	
^{54}Cr	834.85	2^+	100	834.85	2.3(4)	2.9(6)
^{54}Mn	368.29	5^+	99	212.0	1.7(3)[b]	
	407.55	3^+	29	407.5	0.7(4)	
			62	251.2	1.0(3)	
	1009.62	3^+	56	954.9	<0.4	
			44	853.1	<0.3	
	1073.3	6^+	99	704.9	1.2(7)	
	1391.0	1^+	100	1336.0	0.8(5)	
	1454.4	1^+	95	1399.6	0.4(3)	
	1508.40	2^+	67	1508.3	1.7(6)	
^{55}Mn	984.26	$9/2^-$	95	858.2	2.2(4)	3.1(8)
	1289.1	$(11/2^+)$	90	304(2)	<0.4	
	1292.12	$11/2^-$	75	1166.3	0.5(2)	
			25	308.1	hidden	
	1293.0	$(1/2^-)$	100	1293(2)	0.5(5)	
	1528.36	$3/2^-$	97	1528.3	8.8(12)	11.1(11)
	1884.08	$(7/2)^-$	64	1884.0	1.0(7)	
			36	1758.1	0.84(45)	
	2015.2	$7/2^-$	92	1030(2)	<0.3	
	2198.43	$7/2^-$	61	2198.5	0.8(8)	
			33	1213.9	0.5(3)	
	2215.0	$(5/2,7/2)^-$	100	2215(1)	0.5(5)	
	2252.45	$3/2^-$	100	2252.4	2.3(8)	
	2266.89	$(5/2)^-$	73	2268.0	1.5(8)	
			27	739.2	0.8(3)	
	2311.45	$13/2^-$	90	1019.42	<0.25	
	2365.80	$5/2^-$	74	2239.8	1.0(5)	
	2398.41	$\leqslant 9/2^-$	74	2273.1	0.3(3)	
	2426.53	$1/2^+$	100	898.2	2.6(4)	
	2563.15	$3/2^-$	100	2563.0	2.5(8)	
	2727.31	$7/2^-$	52	2727.2	2.1(4)	
			29	1743.0	<0.7	
			19	1435.5	hidden	
	2752.69	$(5/2, 9/2)^-$	24	2752.8	1.1(5)	
			43	2626.7	1.3(6)	
			33	868.6	0.8(4)	
	2873.28	$1/2^-$	23	2873.2	0.9(9)	
			77	1344.8	1.06(30)	
	2976.15	$(3/2–7/2)^-$	77	2976.1	2.2(9)	
			23	1447.3	0.4(4)	
	3037.5	$(1/2,3/2)^-$	100	770.6	1.4(4)	
	3039.9	$(3/2,5/2)^+$	100	2914.1	0.8(6)	
	3424.1	$(3/2)^+$	47	3297.9	0.5(5)	
			53	697.7	0.7(7)	
	3610.8		100	3484.9	<0.5	
^{56}Mn	212.03	4^+	100	212.02	1.7(3)[b]	
	340.99	3^+	93	314.40	hidden	1.3(5)

[a]Present experiment.

[b]There is a transition in ^{54}Mn at 211.99 keV and in ^{56}Mn at 212.026(5) keV. These are too close to distinguish, but at least 70% of the yield must be in ^{54}Mn, because of known cascading from the 1073-keV level.

investigators who could find no (μ^-, ν) transitions in medium to heavy elements. ^{40}Ca seems to be the heaviest nuclide for which such transitions are clearly observed. The reason is probably that most (μ^-, ν) transitions are quite energetic and also the strength is spread out, so no clear identification can be made. (See Fig. 5.2 and the text of Ref. [1] for a discussion of this problem.) The line in ^{54}Cr can also come from ^{54}Mn decay, which is produced in irradiated stainless steel, and the line is detected in other spectra, for example the calcium spectra. However it is much stronger here (and at the right energy), so we believe it is mainly from muon capture [e.g., ^{56}Fe$(\mu^-, \nu pn)^{54}$Cr]. The yield is a little higher than the 2% expected from the systematics of the $(\mu^-, \nu pn)$ reaction, as measured by activation techniques [46], but individual nuclides vary quite markedly.

In Table XIX, we present the yields of the levels in ^{55}Mn. We have assumed that all these levels are produced in the ^{56}Fe$(\mu^-, \nu n)^{55}$Mn reaction and have corrected for the isotopic abundance (91.8%) and removed known cascading.

TABLE XIX. Direct production of levels in ^{55}Mn, from the ^{56}Fe$(\mu^-, \nu n)^{55}$Mn reaction (i.e., Table XVIII values corrected for known cascading and for the isotopic abundance of ^{56}Fe), presented as yield per muon capture, compared to the spectroscopic factors from the ^{56}Fe$(d,^3$He$)^{55}$Mn reaction determined by Puttaswamy *et al.* [12].

Level in ^{55}Mn	Known cascading[a] (%)	Direct yield of level[a] (%)	Spectroscopic factor [12]
0		—	0.11
125.95		—	2.88
984.26	1.5(3)	1.0(6)	
1289.1		<0.4	
1292.12	0.9(2)	−0.1(4)	
1293.0		0.6(6)	
1528.36	5.3(7)	4.3(14)	0.15
1884.08	1.2(4)	0.9(9)	0.07
2015.2		<0.3	
2198.43		1.6(8)	0.38
2215.0		0.6(6)	
2252.45		2.5(9)	
2266.89	1.5(4)	1.2(10)	0.08
2311.45		<0.3	
2365.80		1.5(7)	
2398.41		0.4(4)	
2426.53		2.8(4)	0.84
2563.15		2.7(9)	0.04
2727.31	0.8(8)	3.6(11)	1.72[b]
2752.69		3.6(11)	
2873.28		1.7(3)	
2976.15		2.9(12)	0.17
3037.5		1.5(4)	
3039.9		0.9(7)	0.28, 0.19
3424.1		1.3(13)	0.35
3610.8		<0.6	0.13, 0.09

[a]Present experiment.

[b]Level given as 2727 keV by Puttaswamy *et al.* [12], and comparison to 2741 keV by compilers [10].

We compare these results with the spectroscopic factors from the reaction ^{56}Fe$(d,^3$He$)^{55}$Mn, as observed by Puttaswamy *et al.* [12]. We see that many levels are observed in muon capture, and the match with the spectroscopic factors is not very good. We observe every level with a strong spectroscopic factor, but many other levels are detected too. Unfortunately, there are no (γ, p) data to compare with.

The γ rays in ^{54}Mn are mainly from the reaction ^{56}Fe$(\mu^-, \nu 2n)^{54}$Mn, although a small yield may be from the reaction ^{54}Fe$(\mu^-, \nu)^{54}$Mn, but this isotope has an abundance of only 5.8%, and we do not observe the reaction ^{56}Fe$(\mu^-, \nu)^{56}$Mn. Thus we neglect the contribution from ^{54}Fe and present our results in Table XX as being solely for the reaction ^{56}Fe$(\mu^-, \nu 2n)^{54}$Mn and compare to previous results for the reactions ^{56}Fe$(p,^3$He$)^{54}$Mn [47] and ^{56}Fe$(d, \alpha)^{54}$Mn [48]. The comparison is puzzling; we observe the 1073-keV level more strongly and the 1010-keV level more weakly than these other reactions. Assuming, however, that there is some similar pattern, the other reactions indicate that the ground-state and 55-keV level may be excited in muon capture with a yield of about 2% each.

We may now summarize our observations for iron. Let us assume that all the observed γ rays are from ^{56}Fe, thus raising the yields by 9%. We then find that we observe no γ rays from the (μ^-, ν) reaction; we observe a yield of 36% for the $(\mu^-, \nu n)$ reaction and estimate 4% for the ground-state transition; we observe a yield of 8% for the $(\mu^-, \nu 2n)$ reaction and estimate 2% each for the ground-state and 55-keV levels; and we observe a yield of 4% for the $(\mu^-, \nu 3n)$ reaction. Finally we estimate 5% for all proton and α reactions. Thus we have a grand total of 61%. Now there is probably a significant yield for the 126-keV level in ^{55}Mn (see Table XIX), which may be as large as 5% or even 10%, but there is clearly a lot of remaining unobserved yield, especially from the (μ^-, ν) and $(\mu^-, \nu n)$ reactions, and much of this yield is likely to be producing high-energy γ rays (>3 MeV). These results are compatible with the known neutron multiplicities in muon capture (see Table 4.7 of Ref. [1]). We note that there are unpublished spectra for the reaction ^{56}Fe$(d,^2$He$)^{56}$Mn for a deuteron energy of 172 MeV, with a resolution of 110 keV FWHM [49]. The 0° spectrum shows strong feeding of levels at 110, 1100, 1900, and 2100 keV in ^{56}Mn, but their cross sections fall off fast with angle. We have searched for transitions from such levels but have found no convincing evidence. Our search was complicated by the large level density in ^{56}Mn and the poor information about these levels. We await a full analysis of the 6°–7° bin.

Finally, we present our observed yields for natural nickel in Table XXI and compare these to the results of Evans [11]. In Table XXII, we give the direct production of levels in ^{57}Co and ^{59}Co, taking the cascading into account, and also the isotopic abundances, as well as assuming that the only reactions that occur are ^{58}Ni$(\mu^-, \nu n)^{57}$Co and ^{60}Ni$(\mu^-, \nu n)^{59}$Co. (Natural nickel is 68% ^{58}Ni and 26% ^{60}Ni, with 6% smaller contributions.) Thus the intensities are the values expected for an enriched target of just that isotope. We compare with the spectroscopic factors from the

TABLE XX. Our results for the yields of levels, per muon capture, in the reaction ^{56}Fe(μ^-, $\nu 2n$)^{54}Mn, corrected for the abundance of ^{56}Fe; they are compared to previous results for the reactions ^{56}Fe(p, ^{3}He)^{54}Mn [47] and ^{56}Fe(d, α)^{54}Mn [48]. (We use modern values for the energy levels.)

Level in ^{54}Mn	Known cascading (%)	Direct yield of level in muon capture (%)	Maximum $\sigma(\theta)$ in the (p,^{3}He) reaction	Maximum $\sigma(\theta)$ in the (d, α) reaction
0			58	103
54.87	1.3(6)		40	26
156.3	2.9(5)		3	9.5
368.29	1.3(8)	0.5(8)	20	262
407.55		1.8(5)	4.4	
1009.62		<0.8	44	95
1073.3		1.3(8)	2.5	6.4
1391.0		0.9(5)	50	64
1454.4		0.5(4)	48	34
1508.40		2.8(10)	26	17

^{58}Ni(d,^{3}He)^{57}Co [15,16] and ^{60}Ni(d,^{3}He)^{59}Co reactions [18], which are qualitatively the same as the spectroscopic factors from the ^{58}Ni(t, α)^{57}Co and ^{60}Ni(t, α)^{59}Co reactions [14]. We also compare to the integrated cross sections (in MeV mb) from the ^{58}Ni(γ, $p\gamma$')^{57}Co reaction [13]. The comparisons are quite dramatic; the spectroscopic factors bear only a slight resemblance to our results, but the ^{58}Ni(γ, $p\gamma$')^{57}Co reaction is much closer. Thus the 1378-, 1919.5-, and 2133-keV levels are strongly excited in the (μ^-, νn) and (γ, $p\gamma$') reactions, but not in the (d,^{3}He) reaction. Note that the 1919.5-keV level is not mentioned by Marinov *et al.* [15] nor by Reiner *et al.* [16], but a very small bump appears in the spectrum of Marinov *et al.* on the high-energy edge of the 1897-keV level, though this is probably a resolution effect. In any case the spectroscopic factor is probably <0.05.

TABLE XXI. Yields of γ rays per muon capture in natural nickel, compared with similar data from Evans [11]. (We use level and transition energies as given by the National Nuclear Data Center [10], even if they are illogical, i.e. the transition energy is greater than the level energy.)

Nuclide	Level (keV)	J^π	Transition branching ratio (%)	Transition energy (keV)	Observed γ-ray yield[a] (%)	Observed γ-ray yield [11] (%)
^{56}Fe	846.78	2^+	100	846.77	[b]	9.3(11)
^{57}Co	1223.98	$9/2^-$	100	1224.00	5.6(8)	3.4(12)
	1377.66	$3/2^-$	100	1377.63	5.8(8)	5.9(12)
	1504.83	$1/2^-$	100	127.16	<threshold	
	1689.6	$11/2^-$	46	1689.4	0.7(7)	
			54	465.7	<1.1	
	1757.61	$3/2^-$	99	1757.55	4.0(15)	
	1897.40	$7/2^-$	47	1897.42	1.6(10)	
			53	673.44	2.3(10)	
	1919.50	$5/2^-$	100	1919.52	2.3(8)	
	2133.06	$5/2^-$	83	2133.04	2.3(9)	
			14	755.3	0.3(3)	
^{58}Fe	810.78	2^+	100	810.78	1.7(6)	
^{59}Co	1099.26	$3/2^-$	100	1099.25	4.3(6)	
	1190.45	$9/2^-$	100	1189.6	1.1(8)	
	1291.61	$3/2^-$	93	1291.59	1.6(12)	
	1434.26	$1/2^-$	21	334.8	<0.9	
			79	142.65	<threshold	
	1459.5	$11/2^-$	93	1459.61	<1	
	1481.72	$5/2^-$	76	1481.7	2.6(9)	
			23	382.5	<0.5	

[a]Present experiment.
[b]Too close to the 844-keV line in ^{27}Al.

TABLE XXII. Direct production of levels in ^{57}Co and ^{59}Co from nickel, taking the cascading into account, and also the isotopic abundances, thus the yields, given per muon capture, are for a pure target of the appropriate nickel isotope. We also assume that the only reactions which occur are ^{58}Ni(μ^-, νn)^{57}Co and ^{60}Ni(μ^-, νn)^{59}Co.

Nuclide	Level energy (keV)	Known cascading (%)	Direct yield of level in an isotopic target[a] (%)	Spectroscopic factor [16,18]	Yield in reaction (γ, $p\gamma$') [13] (MeV mb)
^{57}Co	0		nd[b]	5.09	31(8)
	1223.98	4.6(20)	4(2)	0.10	
	1377.66	0.6(2)	8(1)	0.07	30(8)
	1504.83		nd	0.007[c]	nd
	1689.6		<3	0.02	nd
	1757.61		5.9(22)	0.15	10(3)
	1897.40		5.9(19)	1.14	7.7(20)
	1919.50		3.4(12)	nd	11(3)
	2133.06		4.1(16)	0.07	12(3)
^{59}Co	0		nd	3.81	
	1099.26	3(1)	14(3)	0.15	
	1190.45		4.2(27)	nd	
	1291.61		7(5)	0.07	
	1434.26		<16	[d]	
	1459.5		nd	[d]	
	1481.72		10(5)	0.03, 0.22[d]	

[a]Present experiment.
[b]nd: no datum.
[c]See Ref. [5].
[d]This spectroscopic factor has an energy window of 1.4–1.6 MeV.

VII. SUMMARY AND CONCLUSIONS

Our results on muon capture have greatly expanded the information for ^{40}Ca, ^{56}Fe, ^{58}Ni, and ^{60}Ni, and we have presented new information for ^{42}Ca and ^{44}Ca. As with previous investigations, we detect the (μ^-, ν) reaction for ^{40}Ca, but not convincingly for the other targets. This indicates that the strength for the reactions in Fe and Ni is at several MeV and is probably spread among levels that are not well identified in the data compilations. Caurier *et al.* [50] have made calculations for the (n, p) reaction at 0° for several isotopes of Fe and Ni, as well as for V, Mn, and Co. They find that the main 1^+ strength is around 2 MeV in ^{56}Fe and around 3 MeV in ^{58}Ni and ^{60}Ni. Eramzhyan *et al.* [51] calculated muon capture in the nickel isotopes. They found that the 1^+strength is at 5 MeV and a lower yield 1^- strength is between 5 and 10 MeV. However, their nuclear model was the quasiparticle random phase approximation, so it is probably less reliable on the details than the shell-model code of Caurier *et al.*

We observe the (μ^-, νn) reaction strongly for all targets, and it feeds levels in the product nucleus in a similar manner to the (γ, p) reaction for a bremsstrahlung beam of γ rays, with an upper limit of about 32 MeV. (Actually a slightly lower energy may be even better.) The spectroscopic factors for the levels in the product nucleus are a fairly poor predictor, though they are useful for estimating the feeding of the ground state, for which, of course, we have no information.

We also observed other reactions such as the (μ^-, $\nu 2n$) reaction in calcium and iron. Other, more complex, reactions were detected for ^{40}Ca, because we had a much better quality spectrum for the calcium target. As we have explained, ^{40}Ca is also a special case because of the unusual pattern of binding energies in ^{40}K, thus the initiating reaction ^{40}Ca(μ^-, ν)^{40}K* reaches excited states of ^{40}K that can decay only via proton and α emission. For ^{40}Ca, we can account for about 68% of the yield, which is actually quite an achievement in comparison to other nuclei. We hypothesize that the missing strength is about 15% in the (μ^-, ν) reaction, about 15% in the (μ^-, νn) reaction, and 2% for the (μ^-, $\nu 2n$) reaction. For ^{56}Fe, we can account for 65 or 70%, which is just as good. We note that the (μ^-, $\nu 2n$) reaction is much stronger than in calcium, and this trend continues for heavier elements [1]. We hypothesize that for ^{56}Fe we are missing about 15% in the (μ^-, ν) reaction, about 10% in the (μ^-, νn) reaction, and 5% for the (μ^-, $\nu 2n$) and (μ^-, $\nu 3n$) reactions.

Although we have identified the vast majority of the γ rays in our calcium spectra, we note that six are consistently observed with a yield of about 0.3%, yet we have no identification for them. They could, of course, be background lines but are more probably muon capture lines. Their energies are 586, 1145, 1444, 1730.5, 1990, and 3163 keV.

To improve on our data would not be difficult for iron or nickel, although enriched targets would be preferable, and such experiments need about 100 g of target, so only major laboratories can carry the financial risk. For ^{40}Ca, it would be more difficult to improve on our results. Again one would prefer an enriched target, and one would need at least ten times as much data as we obtained, but more importantly there would have to be a major effort to reduce the backgrounds. Tightening the time cuts would help, and also removing extraneous

material from around the target, especially mu-metal and PVC. However, many backgrounds could not be avoided (e.g., thermal neutron capture and inelastic neutron scattering), and it would be necessary to take our approach of taking data on many targets, at least a dozen as we did, and analyzing each with care and perseverance.

ACKNOWLEDGMENTS

We wish to thank the many people who contributed to the successful completion of this experiment: E. Gete, T. P. Gorringe, J. Lange, B. A. Moftah, and M. A. Saliba helped set up the original experiment on nitrogen and took some shifts too. J. Chuma wrote the program PHYSICA, which was used for the data analysis, and also wrote some of the macros specifically for this analysis. Of course in a major laboratory like TRIUMF, many people help by keeping the cyclotron operating and preparing the experimental area for each experiment; the financial contribution for this essential activity is provided by the National Research Council of Canada. Finally we thank the Natural Sciences and Engineering Research Council, Canada, for providing the grants OGP0090780 and 240164-01 that made the experiment possible.

[1] D. F. Measday, Phys. Rep. **354**, 243 (2001).
[2] T. A. E. C. Pratt, Nuovo Cimento B **61**, 119 (1969).
[3] P. Igo-Kemenes, J. P. Deutsch, D. Favart, L. Grenacs, P. Lipnik, and P. C. Macq, Phys. Lett. **B34**, 286 (1971).
[4] T. Chittrakarn, B. D. Anderson, A. R. Baldwin, C. Lebo, R. Madey, J. W. Watson, and C. C. Foster, Phys. Rev. C **34**, 80 (1986).
[5] H. Ullrich and H. Krauth, Nucl. Phys. **A123**, 641 (1969).
[6] J. C. Hiebert, E. Newman, and R. H. Bassell, Phys. Rev. **154**, 898 (1967).
[7] P. Doll, G. J. Wagner, K. T. Knöpfle, and G. Mairle, Nucl. Phys. **A263**, 210 (1976).
[8] D. W. Devins *et al*., Phys. Rev. C **24**, 59 (1981).
[9] P. M. Endt, Nucl. Phys. **A521**, 1 (1990).
[10] www.nndc.bnl.gov ENSDF files.
[11] H. J. Evans, Nucl. Phys. **A207**, 379 (1973).
[12] N. G. Puttaswamy *et al*., Nucl. Phys. **A401**, 269 (1983).
[13] B. S. Ishkanov *et al*., Phys. At. Nucl. **56**, 705 (1993); **56**, 991 (1993).
[14] A. G. Blair and D. D. Armstrong, Phys. Rev. **151**, 930 (1966).
[15] A. Marinov *et al*., Nucl. Phys. **A438**, 429 (1985).
[16] K. Reiner *et al*., Nucl. Phys. **A472**, 1 (1987).
[17] G. Mairle, G. T. Kaschl, H. Link, H. Mackh, U. Schmidt-Rohr, G. J. Wagner, and P. Turek, Nucl. Phys. **A134**, 180 (1969).
[18] G. Mairle, M. Seeger, M. Ermer, P. Grabmayr, A. Mondry, and G. J. Wagner, Nucl. Phys. **A543**, 558 (1992).
[19] T. J. Stocki, D. F. Measday, E. Gete, M. A. Saliba, B. A. Moftah, and T. P. Gorringe, Nucl. Phys. **A697**, 55 (2002).
[20] R. G. Helmer and C. van der Leun, Nucl. Instrum. Methods A **450**, 35 (2000).
[21] E. G. Kessler Jr., M. S. Dewey, R. D. Deslattes, A. Henins, H. G. Börner, M. Jentschel, C. Doll, and M. Lehmann, Phys. Lett. **A255**, 221 (1999).
[22] S. Raman (private communication).
[23] Z. Revay (private communication).
[24] G. Fricke, C. Bernhardt, K. Heilig, L. A. Schaller, L. Schellenberg, E. B. Shera, and C. W. de Jager, At. Data Nucl. Data Tables **60**, 177 (1995).
[25] K. Shizuma, H. Inoue, and Y. Yoshizawa, Nucl. Instrum. Methods **137**, 599 (1976).
[26] Y. Lee, N. Hashimoto, H. Inoue, and Y. Yoshizawa, Appl. Radiat. Isotopes **43**, 1247 (1992).
[27] H. D. Wohlfahrt, E. B. Shera, M. V. Hoehn, Y. Yamazaki, and R. M. Steffen, Phys. Rev. C **23**, 533 (1981).
[28] A. Suzuki, Phys. Rev. Lett. **19**, 1005 (1967).
[29] L. F. Mausner, R. A. Naumann, J. A. Monard, and S. N. Kaplan, Phys. Rev. A **15**, 479 (1977).
[30] F. J. Hartmann, T. von Egidy, R. Bergmann, M. Kleber, H. J. Pfeiffer, K. Springer, and H. Daniel, Phys. Rev. Lett. **37**, 331 (1976).
[31] R. Engfer, H. Schneuwly, J. L. Vuilleumier, H. K. Walter, and A. Zehnder, At. Data Nucl. Data Tables **14**, 509 (1974).
[32] G. Backenstoss, S. Charalambus, H. Daniel, H. Koch, G. Poelz, H. Schmitt, and L. Tauscher, Phys. Lett. **B25**, 547 (1967).
[33] H. L. Acker, G. Backenstoss, C. Daum, J. C. Sens, and S. A. deWit, Nucl. Phys. **87**, 1 (1966).
[34] G. Fricke, J. Herberz, T. Hennemann, G. Mallot, L. A. Schaller, L. Schellenberg, C. Piller, and R. Jacot-Guillarmod, Phys. Rev. C **45**, 80 (1992).
[35] W. J. Briscoe, H. Crannell, and J. C. Bergstom, Nucl. Phys. **A344**, 475 (1980).
[36] T. Suzuki, D. F. Measday, and J. P. Roalsvig, Phys. Rev. C **35**, 2212 (1987).
[37] D. F. Measday at www.physics.ubc.ca/∼measday.
[38] C. van den Abeele *et al*., Nucl. Phys. **A586**, 281 (1995).
[39] G. J. Kramer *et al*., Phys. Lett. **B227**, 199 (1989).
[40] W. K. Collins *et al*., Phys. Rev. C **11**, 1925 (1975).
[41] H. D. Engelhardt, C. W. Lewis, and H. Ullrich, Nucl. Phys. **258**, 480 (1976).
[42] B. Krusche, K. P. Lieb, H. Daniel, T. von Egidy, G. Barreau, H. G. Börner, R. Brissot, C. Hofmayr, and R. Rascher, Nucl. Phys. **A386**, 245 (1982).
[43] T. J. Kennett, M. A. Islam, and W. W. Prestwich, Can. J. Phys. **59**, 93 (1981).
[44] R. Santo, R. Stock, J. H. Bjerregaarde, O. Hansen, O. Nathan, R. Chapman, and S. Hinds, Nucl. Phys. **A118**, 409 (1968).
[45] F. Ajzenberg-Selove and G. Igo, Nucl. Phys. **A142**, 641 (1970).
[46] A. Wyttenbach, P. Baertschi, S. Bajo, J. Hadermann, K. Junker, S. Katcoff, E. A. Hermes, and H. S. Pruys, Nucl. Phys. **A294**, 278 (1978).
[47] A. Guichard, W. Benenson, and H. Nann, Phys. Rev. C **12**, 1762 (1975).
[48] A. R. Majumder, H. M. Sen Gupta, and A. Guichard, Nucl. Phys. **A209**, 615 (1973).
[49] D. Frekers (private communication).
[50] E. Caurier, K. Langacke, G. Martinez-Pinedo, and F. Nowaski, Nucl. Phys. **A653**, 439 (1999).
[51] R. A. Eramzhyan, V. A. Kuz'min, and T. V. Tetereva, Nucl. Phys. **A642**, 428 (1998).